

Fig 2 Correlation of axis electron density with axis velocity (turbulent wakes)

where  $P_\infty$  is the pressure,  $U_\infty$  is the flight velocity, and  $U$  is wake velocity in earth-fixed coordinates (i.e., the velocity defect). As just noted, the  $\text{NO}^+$  population may be considered to be controlled by diffusion alone; hence,

$$\alpha_{\text{NO}^+} \sim U \quad (7)$$

Combining (4-7), there results

$$N_{e-} \sim \frac{U}{1 + C_1 P_\infty (1 + C_2 U)^{-5/2} \exp[C_3/(1 + C_2 U)]} \quad (8)$$

where the various constants and the  $T_\infty$  and  $U_\infty$  dependent terms have been incorporated into  $C_1$ ,  $C_2$ , and  $C_3$ . Therefore, neglecting differences in  $T_\infty$  and  $U_\infty$ , the electron density decay is governed by the velocity decay at a given altitude, i.e., at fixed  $P_\infty$ ,

$$N_{e-}/(N_{e-})^* = F(U/U^*) \quad (9)$$

where  $(N_{e-})^*$  and  $U^*$  are the conditions at the initiation of the attachment effects.

Figure 2 demonstrates the application of Eq (9) to the axis properties of the wakes of a  $10^\circ$  cone ( $R_b = 1$  ft,  $U_\infty = 23,000$  fps) at 120 kft,<sup>10</sup> an  $8^\circ$  cone ( $R_b = 1.5$  ft, 21,500 fps) at 120 kft,<sup>11</sup> and a  $12^\circ$  cone ( $R_b = 0.5$ ,  $M_\infty = 22$ ) at 110 kft.<sup>3</sup> The  $(N_{e-})^*$  and  $U^*$  were taken to be their respective values at the location where the attachment effects have had a 20% effect on the electron density (i.e., the same definition as just used). The data taken from Ref 3 apply to a "model gas" based on oxygen properties; however, air characteristics are accurately reproduced. Considering the differences in flight velocity for the three cases, and that one case applies to a slightly different altitude, the correlation of the data is good.

Although the scaling law is somewhat limited in that it requires the upstream flow properties ( $N_{e-}^*$  and  $U^*$ ) as inputs,<sup>‡</sup> it does help to clarify the details of the final decay of electron population. Furthermore, since the velocity governs the process, the present results emphasize the importance of an accurate representation of the fluidmechanical properties of the downstream wake.

<sup>‡</sup> However, binary scaling is expected to correlate the upstream (recombination-controlled) region.

## References

- Labitt, M., "The measurement of electron density in the wake of a hypervelocity pellet over a six magnitude range," Massachusetts Institute of Technology, Lincoln Lab TR 307 (April 1963).
- Lees, L., "Hypersonic wakes and trails," ARS Paper 2662 62 (November 1962).
- Webb, W. H. and Hromas, L. A., "Turbulent diffusion of a reacting gas in the wake of a sharp nosed body at hypersonic speeds," Space Technology Labs, Ballistic Systems Div TDR-63-138 (April 1963).
- Iien, H., Erdos, J. I., and Pallone, A. J., "Nonequilibrium wakes with laminar and turbulent transport," AIAA Paper 63-447 (August 1963).
- Zeiberg, S. L. and Bleich, G. D., "Finite difference calculation of hypersonic wakes," AIAA Paper 63-448 (August 1963).
- Lin, S. C. and Hayes, J. E., "A quasi one-dimensional model for chemically reacting turbulent wakes of hypersonic objects," AIAA Paper 63-449 (August 1963).
- Chanin, L. M., Phelps, A. V., and Biondi, M. A., "Measurements of the attachment of low-energy electrons to oxygen molecules," Phys Rev 128, 219 (1962).
- Bates, D. R., *Atomic and Molecular Processes* (Academic Press, New York, 1962).
- Nawrocki, P. J., "Reaction rates," Aerophysics Corp of America Rept 61-2-A, Armed Services Technical Information Agency Catalog AD 252534 (1961).
- Zeiberg, S. L., "Wake studies of oxygen-electron attachment and initial conditions," General Applied Science Labs TR 369 (January 1964).
- Hoffert, M., private communication, General Applied Science Labs.

## Tetrahedron Elements in the Matrix Force Method of Structural Analysis

J. S. PRZEMIENIECKI\*

Air Force Institute of Technology, Wright-Patterson  
Air Force Base, Ohio

### Introduction

THE use of solid tetrahedron elements in matrix structural analysis is very attractive, since such elements can be employed in the idealization of solid structural components. The tetrahedron elements so far have been used only in the displacement method of analysis,<sup>1,2</sup> in which the element forces were related to the corresponding displacements through the stiffness matrices determined on the assumption of linearly varying displacements within the tetrahedron. This assumption leads to a compatible, constant stress distribution that also satisfies the stress equilibrium equations within the tetrahedron. Since the stresses vary from element to element, the boundary stress equilibrium will, in general, be violated. The over-all equilibrium of all the elements, however, is maintained through the equilibrium of element forces at common joints, i.e., vertices of the tetrahedra.

The assumption of constant stresses within the element can also be used on the solid tetrahedron to establish its flexibility properties required in the matrix force method of analysis. The flexibility properties of the tetrahedron element may be determined most conveniently for a set of edge force systems acting along the six edges of the tetrahedron. The concept of edge forces was used in Ref 3 to determine flexibility properties of the triangular plate element, where the edge force systems were acting along the three sides of

Received February 17, 1964

\* Associate Professor, Department of Mechanics. Associate Fellow Member AIAA.

the triangle. The concept of edge forces on tetrahedron elements is particularly useful since it leads to very simple flexibility and thermal displacement matrices. These matrices are determined here by the application of the unit load theorem to a set of six independent force systems specified along the six edges of the tetrahedron.

### Independent Force Systems

The six independent force systems  $S_1$ – $S_6$  will be assumed to be located along the edges identified according to Table 1. The numbering  $i$  for the force systems also will be used to specify directions of the edges on which these systems are acting. Sequences other than those given in Table 1 may be selected, but once a sequence has been chosen it must be adhered to throughout the analysis. The force systems  $S_1$ – $S_6$  are shown in Fig. 1. The element forces  $F_1$ – $F_{12}$  used in the matrix displacement analysis<sup>1</sup> are also shown in Fig. 1, and they are related to the forces  $S_1$ – $S_6$  through the following matrix equation:

$$\begin{bmatrix} F_1 \\ F_2 \\ F_3 \\ F_4 \\ F_5 \\ F_6 \\ F_7 \\ F_8 \\ F_9 \\ F_{10} \\ F_{11} \\ F_{12} \end{bmatrix} = \begin{bmatrix} -l_1 & 0 & 0 \\ -m_1 & 0 & 0 \\ -n_1 & 0 & 0 \\ l_1 & -l_2 & 0 \\ m_1 & -m_2 & 0 \\ n_1 & -n_2 & 0 \\ 0 & l_2 & -l_3 \\ 0 & m_2 & -m_3 \\ 0 & n_2 & -n_3 \\ 0 & 0 & l_3 \\ 0 & 0 & m_3 \\ 0 & 0 & n_3 \end{bmatrix} \begin{bmatrix} S_1 \\ S_2 \\ S_3 \\ S_4 \\ S_5 \\ S_6 \end{bmatrix} \quad (1)$$

where  $l_i$ ,  $m_i$ , and  $n_i$  denote here the direction cosines for the directions  $i$ , as specified in Table 1. Equation (1) is used in setting up the equations of equilibrium at each nodal point of the tetrahedron.

If the force system  $S_1$  is applied alone, then an equivalent stress system, in equilibrium with the applied forces, may be taken as a constant tensile stress in the direction of (1). Considering Fig. 2, it is evident that this stress is given by

$$\sigma_1 = 3S_1/A_1 \quad (2)$$

in which  $A_1$  represents area of the projection of the tetrahedron onto a plane normal to the direction (1). The stress  $\sigma_1$  can then be resolved into stress components in the  $x, y, z$  coordinate system. By cyclic changes of subscripts, contributions from other force systems can be obtained, and the results may be expressed by the matrix equation

$$\begin{bmatrix} \sigma_{xx} \\ \sigma_{yy} \\ \sigma \\ \sigma_{xy} \\ \sigma_y \\ \sigma_x \end{bmatrix} = 3 \begin{bmatrix} \frac{l_1^2}{A_1} & \frac{l_2^2}{A_2} & \frac{l_3^2}{A_3} \\ \frac{m_1^2}{A_1} & \frac{m_2^2}{A_2} & \frac{m_3^2}{A_3} \\ \frac{n_1^2}{A_1} & \frac{n_2^2}{A_2} & \frac{n_3^2}{A_3} \\ \frac{l_1 m_1}{A_1} & \frac{l_2 m_2}{A_2} & \frac{l_3 m_3}{A_3} \\ \frac{m_1 n_1}{A_1} & \frac{m_2 n_2}{A_2} & \frac{m_3 n_3}{A_3} \\ \frac{n_1 l_1}{A_1} & \frac{n_2 l_2}{A_2} & \frac{n_3 l_3}{A_3} \end{bmatrix} \begin{bmatrix} S_1 \\ S_2 \\ S_3 \\ S_4 \\ S_5 \\ S_6 \end{bmatrix} \quad (3)$$

or, symbolically in matrix notation,

$$\sigma = \mathbf{a} \mathbf{S} \quad (3a)$$

The direction cosines  $l_i$ ,  $m_i$ ,  $n_i$ , and the areas  $A_i$  can be determined from the location of vertices of the tetrahedron

**Table 1 Location of independent force systems on tetrahedron elements**

Force system or direction $i$	Location (nodal points)
1	1-2
2	2-3
3	3-4
4	4-1
5	1-3
6	2-4

### Flexibility and Thermal Displacements Matrices

The relative displacements  $\mathbf{v}$  for any discrete structural element are given by

$$\mathbf{v} = \mathbf{f} \mathbf{S} + \mathbf{H} \quad (4)$$

where  $\mathbf{f}$  is the flexibility matrix,  $\mathbf{S}$  is the column matrix of element forces, and  $\mathbf{H}$  is the column matrix of relative thermal

displacements. Applying the unit load theorem,<sup>4</sup> the matrices  $\mathbf{f}$  and  $\mathbf{H}$  may be determined from<sup>3</sup>

$$\mathbf{f} = \int_V \mathbf{a}' \mathbf{C} \mathbf{a} dV \quad (5)$$

$$\mathbf{H} = \alpha T \int_V \mathbf{a}' \mathbf{B} dV \quad (6)$$

where, since the tetrahedron is a three-dimensional element,

$$\mathbf{C} = \frac{1}{E} \begin{bmatrix} 1 & -\nu & -\nu & 0 & 0 & 0 \\ -\nu & 1 & -\nu & 0 & 0 & 0 \\ -\nu & -\nu & 1 & 0 & 0 & 0 \\ 0 & 0 & 0 & 2(1+\nu) & 0 & 0 \\ 0 & 0 & 0 & 0 & 2(1+\nu) & 0 \\ 0 & 0 & 0 & 0 & 0 & 2(1+\nu) \end{bmatrix} \quad (7)$$

$$\begin{bmatrix} \frac{l_4^2}{A_4} & \frac{l_5^2}{A_5} & \frac{l_6^2}{A_6} \\ \frac{m_4^2}{A_4} & \frac{m_5^2}{A_5} & \frac{m_6^2}{A_6} \\ \frac{n_4^2}{A_4} & \frac{n_5^2}{A_5} & \frac{n_6^2}{A_6} \\ \frac{l_4 m_4}{A_4} & \frac{l_5 m_5}{A_5} & \frac{l_6 m_6}{A_6} \\ \frac{m_4 n_4}{A_4} & \frac{m_5 n_5}{A_5} & \frac{m_6 n_6}{A_6} \\ \frac{n_4 l_4}{A_4} & \frac{n_5 l_5}{A_5} & \frac{n_6 l_6}{A_6} \end{bmatrix} \begin{bmatrix} S_1 \\ S_2 \\ S_3 \\ S_4 \\ S_5 \\ S_6 \end{bmatrix} \quad (3)$$

and

$$\mathbf{B} = \{1 \ 1 \ 1 \ 0 \ 0 \ 0\} \quad (8)$$

In these equations  $E$  is the Young's modulus,  $\nu$  is the Poisson's ratio,  $\alpha$  is the coefficient of thermal expansion, and  $T$  is the

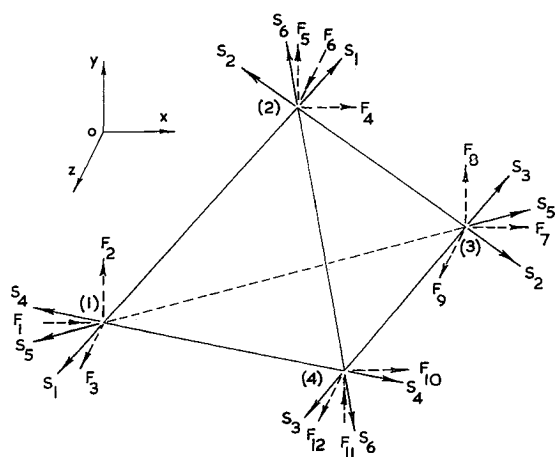


Fig 1 Tetrahedron element

temperature change, which is assumed to be constant over the whole volume of the element

Multiplying out matrices in Eq (5) and then integrating over the element volume, it can be shown that the flexibility matrix

$$\mathbf{f} = [f_{ij}] \quad i, j = 1, 2, \dots, 6 \quad (9)$$

with a typical coefficient

$$f_{ij} = (h_i h_j / EV) \{ (1 + \nu) \cos^2 \theta_{ij} - \nu \} \quad (10)$$

where  $h_i$  represents the length of the edge corresponding to the  $i$ th force system, and  $\theta_{ij}$  is the angle between the  $i$  and  $j$  directions

Similarly, from Eq (6), it can be shown that

$$\mathbf{H} = \alpha T \{ h_1 h_2 h_3 h_4 h_5 h_6 \} \quad (11)$$

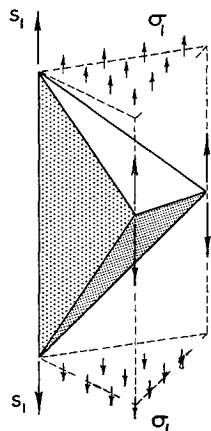
In deriving Eqs (10) and (11), the following equation for the volume of the element was used:

$$V = h_i A_i / 3 \quad i = 1, 2, \dots, 6 \quad (12)$$

A single equation valid for all the  $f_{ij}$  coefficients in the flexibility matrix  $\mathbf{f}$  greatly simplifies the necessary computer programming. Furthermore, the thermal displacement matrix  $\mathbf{H}$  is also easy to evaluate, since it represents simply elongations of the six sides of the tetrahedron caused by the temperature change  $T$ .

### Structural Idealization

The structural idealization based on the concept of constant stress distribution within solid tetrahedron elements can be represented by a three-dimensional pin-jointed framework made up by the sides of tetrahedron elements such that, when adjacent sides of two tetrahedron elements meet, the corresponding framework elements are represented by

Fig 2 Statically equivalent stress distribution due to the force system  $S_i$ 

two parallel pin-jointed bars. However, in contrast to a real pin-jointed framework, where flexibility of each un-assembled bar element is independent of other elements, the flexibilities of bar elements in the idealized framework structure are coupled in sets of six bars representing the six edges of a tetrahedron element.

### References

- Gallagher, R. H., Padlog, J., and Bijlaard, P. P., "Stress analysis of heated complex shapes," *ARS J* **32**, 700-707 (1962).
- Melosh, R. J., "Structural analysis of solids," *J. Struct. Div., Am. Soc. Civil Engrs* **89**, 205-223 (1963).
- Przemieniecki, J. S., "Triangular plate elements in the matrix force method of structural analysis," *AIAA J* **1**, 1895-1897 (1963).
- Argyris, J. H., "Energy theorems and structural analysis," *Aircraft Eng.* **26**, 347-356, 383-387, 394 (1954); **27**, 42-58, 80-94, 125-134, 145-158 (1955); also reprinted (Butterworths Scientific Publications, London, 1960).

## Scattering of Radar Waves by an Underdense Turbulent Plasma

J. MENKES\*

*Institute for Defense Analyses, Washington, D. C.*

IONOSPHERIC physicists have studied the scattering of electromagnetic waves by a turbulent plasma for several years. Some of the earliest contributions to the understanding of the physical principles involved were made by researchers concerned with determining the electron density distribution in the upper atmosphere. Recently, military requirements associated with the re-entry of ballistic missiles have intensified interest in turbulent plasma scattering. This paper extends present understanding of this phenomenon by deriving an experimentally corroborated formula for the radar cross section per unit of plasma volume.

A re-entering ballistic missile leaves an ionized trail, which, like a meteor trail, can be detected by radar. Here we shall assume that current knowledge of the dynamic behavior of the trail or wake must be supplemented only by knowledge of the fluctuations of the dielectric constant of the medium in order to perform the calculations indicated.

If it is assumed that scattering of the incident radiation can be handled by what is commonly called the first Born approximation, then the actual calculation of the radar cross section is essentially a trivial matter. For a given statistical description of the fluctuations of the dielectric constant, the radar cross section is given by an integral, which, if need be, can always be evaluated numerically. With this in mind, we shall concentrate here on the descriptive statistics of the turbulent plasma.

### The Radar Cross Section for a Turbulent Plasma

This discussion assumes that 1) as far as the turbulent fluctuations are concerned, the medium is considered incompressible but not necessarily of constant density, and 2) the turbulence is homogeneous but not necessarily isotropic (boundary effects will thus be neglected).

The dielectric constant of a plasma for the case of negligible absorption is given by

$$1 - \epsilon_0 = \omega_p^2 / \omega^2$$

Presented as Preprint 64-20 at the AIAA Aerospace Sciences Meeting, New York, January 20-22, 1964. The research reported here was supported by the Advanced Research Projects Agency under ARPA Assignment 5, Project DEFENDER.

\* Member, Technical Staff